Electrochimica Acta 196 (2016) 110–117

Contents lists available at ScienceDirect

Electrochimica Acta

journal homepage: www.elsevier.com/locate/electacta

Nafion membranes annealed at high temperature and controlled humidity: structure, conductivity, and fuel cell performance

Bruno R. Matos[a,*], Mauro A. Dresch[a], Elisabete I. Santiago[a], Leticia P.R. Moraes[a], Danilo J. Carastan[b], Jeroen Schoenmaker[b], Ivan A. Velasco-Davalos[c], Andreas Ruediger[c], Ana C. Tavares[c], Fabio C. Fonseca[a]

[a] Instituto de Pesquisas Energéticas e Nucleares, IPEN-CNEN/SP, São Paulo, SP 05508000, Brazil
[b] Universidade Federal do ABC, UFABC, Santo André, SP 09219170, Brazil
[c] Institut National de la Recherche Scientifique—Energie, Matériaux et Télécommunications (INRS-EMT), Varennes, Québec,J3X 1S2, Canada

ARTICLE INFO

Article history:
Received 17 October 2015
Received in revised form 15 February 2016
Accepted 18 February 2016
Available online 22 February 2016

Keywords:
polymer electrolyte fuel cell
membranes
charge transport
microstructure

ABSTRACT

The relationship between electrical and morphological properties of annealed Nafion samples is investigated by X-ray diffraction (XRD), small angle X-ray scattering (SAXS), atomic force microscopy (AFM), and impedance spectroscopy. Experimental data reveal that the heat treatment at high temperature ($T \sim 130$–$140\,^{\circ}C$) with low relative humidity ($RH \sim 0\%$) results in significant changes of Nafion such as increased crystallinity and decreased average distance of hydrophilic domains. Such effects were practically absent when the same heat treatment was carried out at high $RH \sim 100\%$. The effects of annealing with controlled *RH* were reflected in the polymer electrolyte fuel cell (PEFC) tests in which the measured performance was markedly reduced for Nafion samples annealed at low *RH*. Such a feature was related to decreased microstructural stability, water sorption and proton conductivity of the annealed membrane. The observed effects are relevant to evaluate degradation of Nafion during both fuel cell assembly and harsh PEFC operating conditions. Moreover, the experimental results contribute to advance the understanding of Nafion's properties at high temperature for the development of high-performance ionomer membranes.

1. Introduction

Nafion is a leading polymer electrolyte from the family of perfluorosulfonate ionomer membranes (PIM) [1]. PIMs are known to exhibit high chemical/mechanical resistance and, more importantly, one of the highest proton conductivity at low temperatures ($T \sim 80\,^{\circ}C$) among solid proton conductors [2–4]. Owing to such high proton conductivity ($\sigma \sim 10^{-1}\,Scm^{-1}$), PIMs have been extensively used in polymer electrolyte fuel cells (PEFC) to produce high power density output [3].

Optimized operating conditions for PEFC using Nafion have been widely studied. However, further exploring extreme conditions of temperature and/or *RH* is of relevance. One crucial issue that inhibits higher performance is the water management in PEFCs. For example, the excessive amount of water at the fuel cell cathode causes electrode flooding, which slower the diffusion of oxygen towards the catalyst layer [5]. In this scenario, fuel cell tests have been performed at various temperatures and humidity conditions in order to minimize the cathode flooding and maximize the fuel cell performance [5–7]. In fact, due to the excellent mechanical and electrical properties, Nafion has been considered as an electrolyte for PEFCs operating at high temperatures. Among these studies, the development of Nafion-based composite electrolytes for fuel cells at higher temperature and lower relative humidity (*RH*) have received a great deal of attention [5,6,12,15]. The addition of hydrophilic ceramic fillers aims at improving the hydration of the Nafion matrix for PEFC operation at high *T* and low *RH* [4,5]. However, relatively little attention has been given to changes of Nafion morphology at such conditions, which can decrease the membrane conductivity and, consequently, the fuel cell performance [4,6,15]. Several factors are involved in the reduction of the proton conductivity of Nafion at high *T* and low *RH* such as the loss of absorbed water, the increase of the membrane crystallinity, and the thermal transitions of the ionic phase [3,13,14].

Nafion properties have been widely studied and several models have been proposed to account for the relationship between the morphology, mechanical, and electrical properties [1,9]. However,

* Corresponding author.
E-mail address: brmatos@usp.br (B.R. Matos).

http://dx.doi.org/10.1016/j.electacta.2016.02.125
0013-4686/

the available models considered experimental data collected in a limited temperature range (mostly, from room temperature to 80 °C). In this low temperatures, below the α-transition of Nafion at $T\alpha$ ~110 °C, changes on the ionomer's properties such as crystallinity and proton conductivity are negligible [1,4]. Indeed, high temperature characterization of Nafion crystallinity has been performed mostly in dry conditions, hampering the application of models to describe the role of the water at $T > T\alpha$. Therefore, such models do not reflect the PEFC operating conditions, requiring new efforts to understand the relation between the morphology and electrical properties of PIMs at high temperature and different relative humidity [6–8].

Concerning the morphology of Nafion, it has been confirmed by several techniques that the sulfonic acid groups form ionic clusters and that the tetrafluorethylene (TFE) segments of the main chains crystallize during the fabrication process, such as extrusion (lamination) or casting. Both ionic and nonionic phases are nanometer sized and are ubiquitously distributed in the polymer matrix [1]. In this framework, two processes are likely to occur at high T: the crystallization of the TFE segments and the conformational changes of the polymeric aggregates, changing both ionic and nonionic domains of Nafion. The influence of ionic and nonionic phases on α-transition have been a subject of debate for several decades [9,10]. For example, the endotherm peak at ~130 °C, observed in differential scanning calorimetry runs of Nafion, was attributed to the melting of ill-formed crystallites allowing for the growth of a more crystalline phase [9]. In contrast, such a peak has also been assigned to the conformation changes of Nafion backbone due to electrostatic interactions [11]. Therefore, the understanding of the morphology changes of Nafion at low *RH* and high T is important for controlling the main properties that maximize the PEFC performance in such conditions. Moreover, the study of the microstructure of ionomer membranes at conditions that mimic the fuel cell operating conditions, using more suitable techniques for assessing changes of the morphology of PIMs, such as atomic force microscopy (AFM) and small angle X-ray scattering (SAXS) are scarce.

In this study, the influence of both thermal and humidification history of Nafion membranes on the performance of PEFCs was investigated. The results indicated that at low *RH* and at $T > T\alpha$, crystallization of the TFE moieties of the polymer backbone and destabilization of the hydrophilic domains takes place, contributing for decreasing both the proton conductivity and the performance of the fuel cell. On the other hand, the crystallization of samples annealed at high *RH* was inhibited, a feature that resulted in a lower reduction of the proton conductivity, as compared to the sample annealed at low *RH*, and allowed reaching enhanced PEFC performance.

2. Experimental

Commercial Nafion membranes with different equivalent weight (EW), Nafion 105 (EW = 1,000 g eq^{-1}) and 115 (EW = 1,100 g eq^{-1}) were obtained from Dupont. The membranes were post-treated in three different solutions: HNO_3 (7 mol L^{-1}), H_2O_2 (3 vol. %), and H_2SO_4 (0.5 mol L^{-1}) at 80 °C for 1 h, with intermediate washing steps with deionized water for organic solvent residues removal and to assure the protonic (H^+) form of the polymeric matrix.

PEFC measurements using Nafion membranes at low *RH* followed two protocols: *i)* the PEFC was stabilized for 2 h at high *RH* (*RH* = 100%/T = 130 °C) followed by a decrease of the *RH* to 50%; and *ii)* the PEFC was stabilized for 2 h at low *RH* (*RH* = 40%/T = 130 °C) followed by an increase of the *RH* to 100%. Results of PEFC testing were combined with AFM, XRD and SAXS characterizations of annealed samples at temperatures above α-transition ($T\alpha$ ~110–120 °C), both at *RH* = 100% and *RH* ~0%.

Membrane electrode assemblies (MEAs) with 5 cm^2 area, were fabricated by hot pressing electrodes onto N115 and N105 membranes at 125 °C and 1000 kg fcm^{-2} for 2 min. The detailed preparation of gas diffusion electrodes and MEAs has been described elsewhere [12]. Electrodes were prepared by filtration and brushing procedures. The filtration consisted of filtering under vacuum a mixture of a Teflon suspension and carbon powder (Vulcan XC-72) on both faces of the carbon cloth substrate to form the diffusion layer (GDL). The resulting GDL is cured in a resistive furnace at 300 °C for 30 min. The catalyst layer is added to GDL by brushing an ink of Pt/C catalyst (~0.4 mg cm^{-2}/E-Tek) and a Nafion 5 wt% solution (Dupont). The resulting electrode was placed in an oven at 80 °C for 24 h. The polarization curves (I–V) were taken at 130 °C. The system was stabilized and conditioned by draining electrical current at a fixed voltage of 0.7 V for 2 h before data collection in order to reach steady state. The gases were saturated with water by using gas humidifiers. The reactant gases, O_2 and H_2, were water saturated by passing them through humidifiers set at the same temperature of the cell. Fuel cells were fed with hydrogen and oxygen at flow rates of 440 mL min^{-1} and 380 mL min^{-1}, respectively. All experiments were performed under an absolute pressure of 3 bar to ensure *RH* = 100%. For measurements under low *RH* at 130 °C, reduced *RH* conditions (40% < *RH* < 100%) were set by reducing the temperature of gas humidifiers with respect to the fuel cell temperature, using Eq. (1). In this case, T_r and T_c correspond to humidifier and fuel cell temperature, respectively.

The proton conductivity of the membranes was measured by impedance spectroscopy (IS) using a frequency response analyzer (Solartron 1260) and a homemade airtight sample holder with through-plane carbon cloth terminal leads and a K-type thermocouple [2]. The sample holder is based on two connected stainless steel chambers, the upper sample chamber and a water reservoir below, separated by a thermal insulator Teflon ring that allows independent temperature control of each chamber [2,6]. Temperature controllers connected to band heaters placed externally around the cylindrical chambers are monitored by thermocouples (type K) inserted inside the metallic walls. The constructed sample holder is capable of controlling both T (from room temperature up to ~200 °C) and the *RH* (from ~3 to 100%). Nafion samples were sandwiched between stainless steel spring-load contact terminals (insulated from the chamber walls) with carbon cloth to facilitate water equilibration. Similarly to PEFC tests, this experimental apparatus, the *RH* of the sample chamber can be calculated by:

$$RH = \rho(T_r)/P(T_c)x100 \quad (1)$$

here ρ is the saturated vapor partial pressure, P is the vapor partial pressure, and T_r and T_c are, respectively, the water reservoir and sample chamber temperatures. Two-probe IS measurements were performed in the 40–180 °C temperature range, in the 4 mHz to 1 MHz frequency interval, with 100 mV applied amplitude. The interfacial resistance between electrodes and the membrane were subtracted in accordance with previous reports [2]. The impedance spectroscopy measurements were performed on Nafion membranes annealed at two conditions: *i*) samples were annealed in oven (dry environment) for 2 h at 130 °C; and *ii*) the wet samples were annealed for 2 h at 130 °C at *RH* = 100%.

The water uptake was obtained for the as-received and annealed samples by the relative gain of liquid water with respect to the dry sample. The dry weights of the as-received sample and the sample annealed at *RH* = 100% (T = 130 °C) were obtained previously the heat-treatment. These samples were dried at ~80 °C

for 30 min in order to minimize annealing effects. The wet weights for the as-received and annealed samples were obtained after 24 h of immersion in deionized water at room temperature.

Small angle X-ray scattering (SAXS) experiments were carried out using synchrotron radiation at the SAXS beamline of the Brazilian National Synchrotron Light Laboratory (LNLS). Experiments were conducted with an incident wavelength λ = 1.488Å in the range of the scattering vector q ~0.02–0.35 $Å^{-1}$ ($q = 4\pi \sin\theta/\lambda$, being 2θ the scattering angle). Scattering patterns were collected with MarCCD detector and the intensity curves were corrected for parasitic scattering, integral intensity, and sample absorption. SAXS measurements of fully swollen samples were carried out after immersing the membranes in deionized water for 24 h. For the study of the annealing temperature in the sample morphology, SAXS measurements were performed on samples annealed in dry and humid atmospheres. The annealing of Nafion samples in dry atmosphere was carried out in an oven for 2 h at 140 °C at reduced relative humidity (*RH* ~0%). At constant partial pressure of water at 140 °C, the relative humidity of the oven is pronouncedly reduced. The annealing in humid atmosphere was performed by placing Nafion samples in the conductivity chamber for 2 h at 140 °C and at *RH* = 100%. For the sake of clarity of the discussion, the humid and dry conditions samples will be labelled *RH* = 100% and *RH* ~ 0%, respectively. After the heat treatments, both samples were positioned in the sample-holder at room temperature and ambient *RH* for SAXS measurements. For SAXS measurements as a function of temperature, N105 and N115 samples were positioned in a special sample-holder, consisting of a metallic clamps coupled with a resistive heating. The sample-holder has a ~3 mm window for the X-ray beam and the measurements were performed in the 30–160 °C *T*-range.

X-ray diffraction data were collected on membranes from 2θ ~10–60°, at a scanning rate ~2.0 $2\theta°\ min^{-1}$ a Bruker diffractometer, operating in the transmission mode, using CuKα radiation (λ = 1.54056 Å).

Atomic force microscopy (AFM) experiments were carried out on an AIST-NT SMART microscope in intermittent (tapping) mode. A sharp silicon beam-deflection cantilever was used with an oscillation amplitude around 10 nm and a set point that was optimized for a large phase contrast. Observations were conducted on multiple areas to confirm both the uniformity and the reproducibility of the encountered experimental conditions.

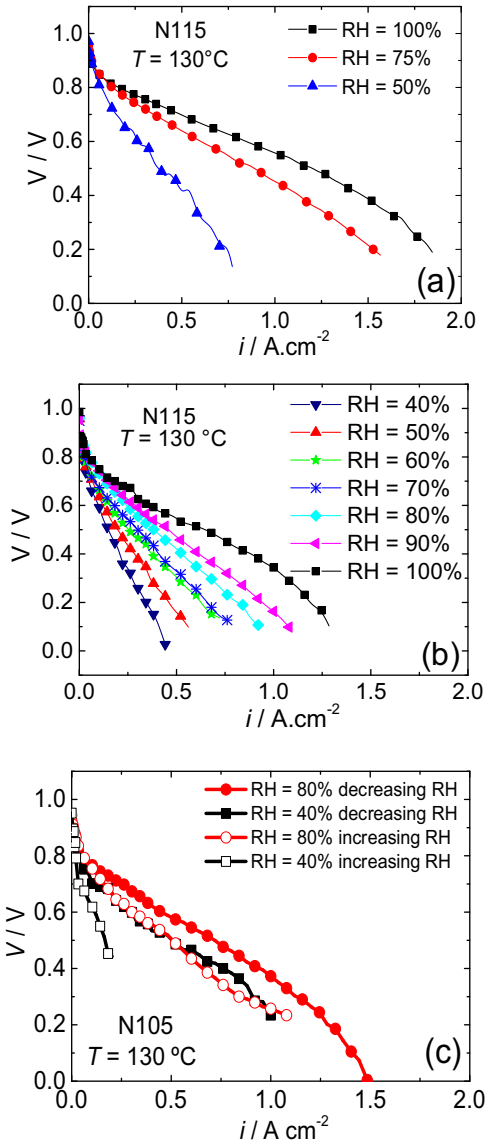

Fig. 1. (a) Polarization (*I*–*V*) curves of PEFC using N115 as electrolyte at 130 °C with *decreasing* relative humidity; (b) Polarization curves of PEFC using N115 as electrolyte at 130 °C with *increasing* relative humidity; and (c) Polarization curves of PEFC using N105 as electrolyte at 130 °C with *decreasing* and *increasing* relative humidity.

AFM topology images were obtained at 25 °C for Nafion samples annealed *in situ* at 140 °C for 2 h at *RH* ~ 0%. Rectangular films were cut respecting the extrusion direction (machine direction) and positioned vertically in the substrate surface. The AFM topology images of the samples annealed at *RH* = 100% (Fig. 5**e** and **f**) have been performed using an Agilent AFM/SPM Series 5500 in ACAFM (tapping mode).

3. Results and Discussion

Fig. 1 shows the effect of the two annealing protocols on the PEFC performance investigated during fuel cell operation. Fig. 1**(a)** shows the PEFC *I–V* curves at 130 °C of N115 measured at different relative humidity. Prior to recording polarization curves, the fuel cell was conditioned at 130 °C for 2 h at *RH* = 100% to fully hydrate the membrane. Then, measurements were performed by gradually decreasing the *RH*. The *I–V* curves at *T* = 130 °C exhibit a significant performance loss for *RH* < 100%. The decrease of the fuel cell performance is more pronounced when *RH* is reduced from 75% to 50%. Such decrease is mainly observed in the linear portion of the polarization curve indicating that the low *RH* decreased the water content of the electrolyte, resulting in a reduction of the proton conductivity [5,12]. This result is in agreement with previous proton conductivity data as a function of *RH*, which showed a pronounced decrease of the proton conductivity of Nafion for *RH* < 60% [16].

The polarization curves of N115 membranes, obtained as a function of *RH* at *T* = 130 °C, after preconditioning the fuel cell for 2 h at reduced *RH* = 40%, exhibit a different behavior. Fig. 1**b** shows the *I–V* curves taken at 130 °C with increasing *RH*. Fig. 1**(b)** shows that the performance of fuel cells conditioned at low *RH* are significantly lower than the ones preconditioned at *RH* = 100%, shown in Fig. 1**(a)**. It is interesting to note that the performance degradation observed by decreasing *RH* from 100% to 75% in Fig. 1**(a)** is lower than the one observed by decreasing *RH* from 100 to 70–80% in Fig. 1**(b)**. This result strongly suggests that the membrane conditioned during the fuel cell tests at *T* = 130 °C with low *RH* (Fig. 1(b)) exhibits a lower water sorption capacity and lower proton conductivity, as inferred from the higher slope of *I–V* curves at *RH* < 100%.

The influence of the *RH* on the annealing of Nafion was also investigated for N105 membranes. Fig. 1**(c)** shows the PEFC measurements for N105 performed at both increasing and decreasing *RH* at 130 °C, following the same annealing protocol of N115 (Fig. 1(a) and (b)). Tests of N105 PEMFC at *RH* = 100% (not shown) exhibited lower performance than at *RH* = 80%, indicating that N105 requires an optimized protocol for fuel cell testing [17,18]. Nevertheless, Fig. 1**(c)** shows that N105 has similar behavior of N115, i.e., the PEFC performance is affected by both the thermal and *RH* history of the PEFC. Annealing the fuel cell at *T* = 130 °C with *RH* = 100% causes lower performance degradation than annealing at *RH* = 40%. Such degradation is evident in the ohmic drop portion of *I–V* curves, indicating that such an effect is mostly related to the PIM electrolyte.

Proton conductivity measurements of both as-received membranes and samples annealed at *RH* ~0% and *RH* = 100% can reveal the effect of the annealing conditions on the electrolyte performance during fuel cell operation. Fig. 2 shows the proton conductivity data measured at *RH* = 100% for N115 (a) and N105 (b) samples previously annealed (*T* = 130 °C) at *RH* ~0% or 100%.

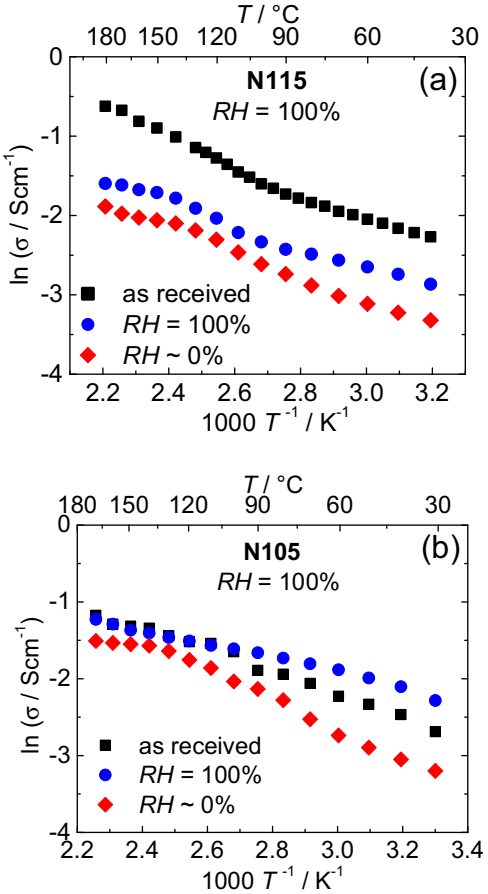

Fig. 2. Temperature dependence of the proton conductivity at *RH* = 100% of N115 (a) and N105 (b) previously annealed in humid and dry environments.

Conductivity data at *RH* = 100% shown in Fig. 2 revealed a thermally activated proton transport in the entire *T*-range studied ($40 < T < 180$ °C). Annealed N115 samples (Fig. 2**(a)**) displayed considerably lower proton conductivity than the as-received sample. Moreover, the proton conductivity of the sample annealed at *RH* ~0% is lower than the sample annealed at *RH* = 100%. For N105, the proton conductivity of annealed samples exhibits similar behavior, i.e., annealing at *RH* ~0% decreases the conductivity more pronouncedly than annealing at *RH* = 100%. However, the conductivity of N105 is less dependent on the annealing than in N115 samples. More significant differences are observed at $T \leq 100$ °C, in which the conductivity of the as-received N105 is lower than that of the sample annealed at *RH* = 100%. Thus, the results of Fig. 2 show that the lower PEFC performance for the samples annealed at lower *RH* (Fig. 1) is mainly an outcome of the lower proton conductivity of such PIM's.

The water content of annealed Nafion samples was measured to further investigate the properties associated with the reduced proton conductivity. The water content of as-received N115 and samples annealed at *T* = 130 °C with *RH* ~0% and at *RH* = 100% are ~33 wt%, 19 wt%, and 45 wt%, respectively. For N105, the water content of samples annealed at *RH* = 100% is ~65 wt%, a value considerably higher than the water content of both the as-received (~36 wt%) and the sample annealed at *RH* ~0% (~26 wt%). The larger water content in N105 is in agreement with the lower equivalent weight, as compared to N115, which provides more active ionic sites for water sorption. Nevertheless, the differences observed in the proton conductivity cannot be exclusively attributed to the higher water content of samples annealed at *RH* = 100%. The proton conductivity of as-received N115 [$\sigma(T = 130$ °C) ~0.33 S cm^{-1}] is higher than that of N105 [$\sigma(T = 130$ °C) ~ 0.24 S cm^{-1}]. However, at 130 °C after the annealing at *RH* ~0% N105 and N115 conductivity are σ ~0.19 S cm^{-1} and ~0.11 S cm^{-1}, respectively. Such values evidence that N115 annealed at *RH* ~0% has a more pronounced decrease of the conductivity (Fig. 2), possibly related to the reduced water content (19 wt%).

The observed effects of annealing with controlled *RH* on the fuel cell performance, proton conductivity, and water content are possibly related to structural changes of Nafion. In order to evaluate the changes of the PIM structure upon annealing, SAXS and XRD measurements were carried out as shown in Fig. 3.

Fig. 3**(a)** shows the XRD patterns of N105 annealed at *T* = 140 °C with both *RH* ~0% and 100%. In Fig. 3**(a)**, all samples exhibited the characteristic amorphous halo at 2θ ~16.2°. However, the sample annealed at *RH* ~0% presented a distinct peak at 2θ ~17.5°, which was assigned to the ordering of TFE crystals [1]. Such a peak is a clear evidence of a higher degree of crystallinity of the sample annealed at *RH* ~0%. On the other hand, no change of the diffraction peak of N105 annealed at *RH* = 100% was detected. Such a result strongly indicates that the presence of water inhibits the polymer crystallization at high temperature [19].

Fig. 3**(b)** shows SAXS patterns collected at ambient conditions of N105 annealed at *T* = 140 °C both at *RH* ~0% and *RH* = 100%. Usually, SAXS patterns of nearly dry Nafion membranes display two scattering maxima centered at *q* ~1.9 nm^{-1} (ionomer peak) and at *q* ~0.5 nm^{-1} (matrix peak) [19]. The ionomer peak is attributed to the correlation distance among elongated polymeric aggregates, whereas the matrix peak is related to the long-range correlations among lamellar Teflon-like crystals [19]. Such peaks can be clearly observed in Fig. 3**(b).** The SAXS pattern of N105 annealed at *T* = 140 °C and *RH* ~0% (Fig. 3**(b)**) shows a higher intensity of the matrix peak with respect to the sample annealed at *RH* = 100%. Such an increased correlation indicates a higher crystallinity of the sample annealed at *RH* ~0%, in agreement with XRD data (Fig. 3**(a)**). In addition, the ionomer peak for the sample annealed in dry condition is slightly shifted to higher *q*-values. The *d*-spacings ($d = 2\pi/q$) calculated for Nafion samples annealed at *RH* ~0% and *RH* = 100% are ~3.4 and ~3.7 nm,

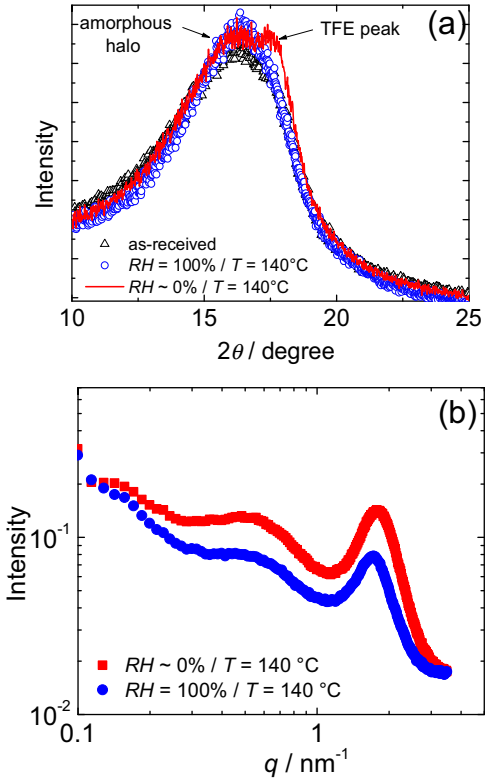

Fig. 3. (a) XRD for N105 samples annealed in dry condition and at *RH* = 100%; and (b) SAXS patterns for N105 annealed in dry condition and at *RH* = 100%.

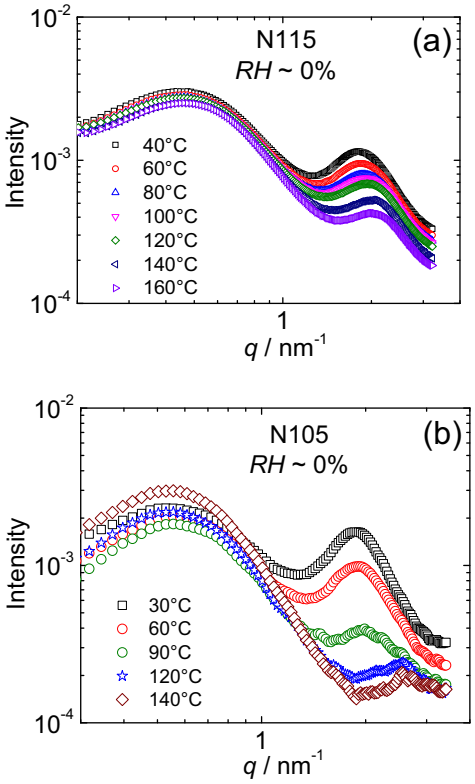

Fig. 4. (a) SAXS patterns measured in the 40–160 °C temperature range for N115; and (b) SAXS patterns measured in the 30–140 °C temperature range for N105.

respectively. Such reduction of the hydrophilic domains spacing may be linked to the reduced water sorption of samples annealed at *RH* ~0%.

The structural changes of Nafion can be better evaluated in SAXS measurements taken upon heating shown in Fig. 4 for both N115 and N105. Fig. 4**(a)** and **(b)** show SAXS measurements of N115 and N105, respectively, with increasing temperature at *RH* ~0%. In Fig. 4**(a)** and **(b)**, it can be observed a concomitant decrease of intensity and a shift of the ionomer peak to higher *q*-values with increasing temperature for both N105 and N115 samples. The intensity of the matrix peak of N115 remains nearly constant up to 160 °C. Unlike the N115 sample, Fig. 4**(b)** shows that the scattering intensity of crystallites of N105 increases for $T > 90$ °C. The high-*q* shift of the ionomer peak for N105 occurring from ~2.0 nm^{-1} (90 °C) to ~2.6 nm^{-1} (140 °C) indicates a significant reduction of the correlation distance of the hydrophilic domains from ~3.1 nm to ~2.4 nm as the temperature increases. The reduction of the correlation distance measured for the N115 sample is lower than that for N105, there being ~3.3 nm at 80 °C and ~2.9 nm at 140 °C.

Recent SAXS analyses (solutions and membranes) have indicated that the morphology of Nafion consists of an electrostatically crosslinked collection of fibrillar polymeric aggregates [19]. Therefore, the larger concentration of ionic groups in N105, as compared to N115, may result in differences of ionic groups ordering. The ionomer peak is a result of the electron density contrast existing between the hydrophilic and hydrophobic phases [19]. Hence, the intensity decrease and broadening of the ionomer peak for both N105 and N115 samples as the temperature increases can be related to a reduction of the water content and a lower ordering between the ionic domains [19]. Both the morphology and water content have a direct influence on the decreased proton conductivity of the samples. On the other hand, the increase of scattering intensity of the matrix peak suggests that a reorganization of Nafion crystallites occurs with increasing temperature, as observed in the SAXS patterns of N105 at $T > 90$ °C. These results indicate a higher ordering of the crystalline phase of the annealed samples. However, the absence of changes in the intensity and shape of the matrix peak of N115 suggests that the crystallinity is not altered during annealing at $T < 160$ °C.

The structural changes observed for N105 and N115 influence both the water sorption capacity and the proton conductivity of the PIM's. However, it is difficult to understand the changes observed in the proton conductivity of the annealed samples in terms of the structural data since the water sorption capacity changes concomitantly. Nonetheless, it is important to note that the most pronounced changes in the water sorption capacity, proton conductivity and structural data were observed at high temperatures ($T > T\alpha$), suggesting that the thermal transitions of the ionomer is the main factor that triggers the structure/property changes. The marked behavior observed for N105, observed at a lower temperature than N115, adds further evidence that the ionomer structural changes may be associated with thermal transitions of the hydrophilic phase (α-transition). Previous reports showed that the α-transition of N105 and N115 occurs at $T\alpha$ ~80 °C and $T\alpha$ ~120 °C, respectively [3], indicating that the N105 has a less stable structure. Above the α-transition, it has been reported that the ionic interactions that hold the ion conducting network stable is weakened, a feature that may trigger the reorganization of Nafion structure to a more crystalline state. In N105, the larger number of ionic groups (lower equivalent weight) results in higher water sorption, which destabilizes the ionic interactions and decreases the temperature of α-transition, as compared to N115.

Therefore, the annealing of Nafion samples in dry atmospheres at $T > T\alpha$ imposes a significant change of the ionomer structure, which is related to the observed decrease of both the proton conductivity and the PEFC performance. It is worth noting that the proton conductivity at high temperature of N105 annealed at

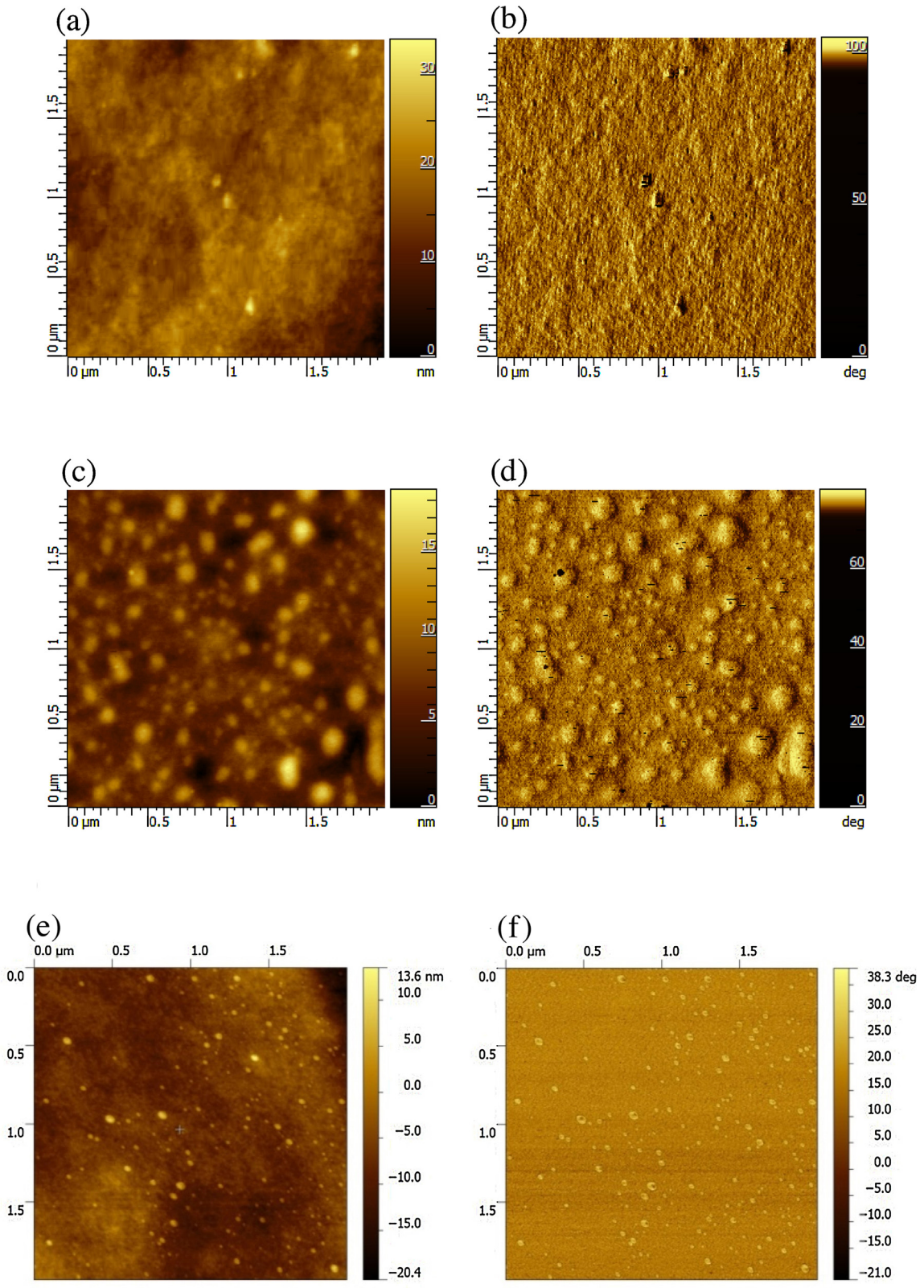

Fig. 5. AFM topography (left) and phase (right) images of the N105 samples: (**a** and **b**) non-annealed; (**c** and **d**) annealed at $T = 140\,^{\circ}C$ in dry condition; and (**e** and **f**) annealed at $T = 140\,^{\circ}C$ in humid condition.

different *RH* are comparable, irrespective of the observed differences of crystallinity, as inferred form XRD and SAXS data. Such a result indicates that crystallinity is not affecting the transport properties of water-swollen Nafion membranes, further suggesting that the ionic phase plays a predominant role for the charge transport. Nevertheless, a clear separation between the effects due to changes in crystallinity and ionic domains upon heating is a hard task that is beyond the scope of the present study.

In order to further evaluate morphological changes of membranes annealed at $RH = 100\%$ and $RH \sim 0\%$, surfaces of N105 membranes were studied by AFM as shown in Fig. 5. The AFM topography and phase images show a large fraction of bright spherical features at the surface of the samples annealed at $T \sim 140\,^{\circ}C$ in dry conditions. On the contrary, for both as-received and the sample annealed at $RH = 100\%$ only a very small amount of such bright structures are observed. These protrusions were previously observed and were attributed to the non-ionic domains composed mainly of TFE hydrophobic segments of the ionomer chains [20,21]. The presence of bright protrusions in the sample annealed at $RH \sim 0\%$ is in agreement with SAXS and XRD data, and suggests that the bright spots are possibly associated with the growth of crystalline domains at high temperatures.

It is worth noting that the AFM and SAXS analyses evidence that the distinction between the role played by both crystallinity and ionic domains to the electric properties of Nafion can be performed for samples annealed at $RH = 100\%$, which have not exhibited noticeable changes on the ionomer crystallinity. The increase of the ionomer crystallinity in Nafion samples annealed at dry conditions was observed by different authors [4,9,22,23,24]. However, annealing also promotes changes on both the ionomer water content and the ordering of the ionic domains, which inhibits an unequivocal attribution of the main factor affecting the charge transport properties of Nafion [25]. Nonetheless, the combined study of the water uptake, proton conductivity, and structural analysis suggests that the most pronounced effect reducing the conductivity of both N105 and N115 is related to irreversible structural changes, mainly associated with the hydrophilic domains of the membrane. Possibly, the ionic domains of Nafion are irreversibly deformed at $T > T\alpha$, an effect intensified at lower RH. Therefore, the decrease of fuel cell performance observed for $RH < 100\%$ in Fig. 1 occurs probably because irreversible transitions of the ionic domains inhibit the recovery of the polymer structure that affects swelling and water absorption. It is worth noting that the results shown in Figs. 4 and **5** suggest that the hot-pressing of Nafion-based membrane-electrode assembly (MEA), which is a typical step carried out at $T > T\alpha$ in dry conditions during PEFC fabrication is likely to promote significant degradation of the electrical properties of the PIM.

4. Conclusions

The effect of the relative humidity during the annealing of Nafion samples at temperatures higher than the α-transition was studied. Experimental results indicated that at low relative humidity and high temperatures, the ionomer membranes may exhibit higher level of crystallinity and decreased average spacing of the hydrophilic domains. The predominant factors reducing the proton conductivity and the fuel cell performance at high temperature and low relative humidity are attributed to such structural changes and to decreased water sorption capacity of annealed samples, which were possibly triggered by thermal transitions of the ionomer. On the other hand, experimental results revealed that properties of samples were significantly less affected when the annealing was carried out at high relative humidity. The preconditioning of the sample at high T and high RH allowed obtaining a higher PEFC performance. These results are important for understanding the role of the thermal history for the MEA preparation and for the use of Nafion membranes at high temperatures.

Acknowledgement

Thanks are due to the Brazilian agencies for scholarships and funding: CNEN, CAPES (BRM), CNPq (EIS and FCF), and FAPESP 2013/50151-5 (BRM), 2015/11967-5 (LPRM), 2014/50279-4, 2014/09087-4. This work was carried out with partial financial support of the Natural Sciences and Engineering Research Council of Canada and the Canadian Foundation for Innovation.

References

[1] A. Eisenberg, J.-S. Kim, Introduction to Ionomers, 1 Ed., Wiley-Interscience, 1998.
[2] B.R. Matos, C.A. Goulart, E.I. Santiago, R. Muccillo, F.C. Fonseca, Proton conductivity of perfluorosulfonate ionomers at high temperature and high relative humidity, Appl. Phys. Lett. 109 (2014) 091904.
[3] B.R. Matos, E.I. Santiago, R. Muccillo, I.A. Velasco-Davalos, A. Ruediger, A.C. Tavares, F.C. Fonseca, Interplay between α-relaxation and morphology transition of perfluorosulfonate ionomer membranes, J. Power Sources 293 (2015) 859.
[4] M.K. Mistry, N.R. Choudhury, N.K. Dutta, R. Knott, Nanostructure Evolution in High-Temperature Perfluorosulfonic Acid Ionomer Membrane by Small-Angle X-ray Scattering, Langmuir 26 (2010) 19073.
[5] E. Chalkova, M.V. Fedkin, S. Komarneni, S.N. Lvov, Nafion/Zirconium Phosphate Composite Membranes for PEMFC Operating at up to 120 °C and down to 13% RH, J. Electrochem. Soc. 154 (2007) B288.
[6] F. Bauer, M. Willert-Porada, Characterisation of zirconium and titanium phosphates and direct methanol fuel cell (DMFC) performance of functionally graded Nafion(R) composite membranes prepared out of them, J. Power Sources 145 (2005) 101.
[7] M.B. Satterfield, J. Benziger, Viscoelastic properties of Nafion at elevated temperature and humidity, J. Polym. Sci.: Part B: Polym. Phys. 47 (2009) 11.
[8] B.R. Matos, M.A. Dresch, E.I. Santiago, M. Linardi, D.Z. de Florio, F.C. Fonseca, Nafion β-Relaxation Dependence on Temperature and Relative Humidity Studied by Dielectric Spectroscopy, J. Electrochem. Soc. 160 (2013) F43.
[9] K.A. Page, K.M. Cable, R.B. Moore, Molecular Origins of the Thermal Transitions and Dynamic Mechanical Relaxations in Perfluorosulfonate Ionomers, Macromolecules 38 (2005) 6472.
[10] S.C. Yeo, A. Eisenberg, Physical properties and supermolecular structure of perfluorinated ion-containing (nafion) polymers, J. Appl. Polym. Sci. 21 (1977) 875.
[11] Y. Kawano, S.H. Almeida, Thermal Behavior of Nafion Membranes, J. Therm. Anal. Calor. 58 (1999) 569.
[12] B.R. Matos, R.A. Isidoro, E.I. Santiago, F.C. Fonseca, Performance enhancement of direct ethanol fuel cell using Nafion composites with high volume fraction of titania, J. Power Sources 268 (2014) 706.
[13] M.-H. Kim, C.J. Glinka, S.A. Grot, W.G. Grot, SANS Study of the Effects of Water Vapor Sorption on the Nanoscale Structure of Perfluorinated Sulfonic Acid (NAFION) Membranes, Macromolecules 39 (2006) 4775.
[14] Z. Gadjourova, Y.G. Andreev, D.P. Tunstall, P.G. Bruce, Ionic conductivity in crystalline polymer electrolytes, Nature 412 (2001) 520.
[15] G. Alberti, M. Casciola, L. Massinelli, B. Bauer, Polymeric proton conducting membranes for medium temperature fuel cells (110–160 °C), J. Mem. Sci. 185 (2001) 73.
[16] B.R. Matos, E.I. Santiago, F.C. Fonseca, Irreversibility of Proton Conductivity of Nafion and Nafion-Titania Composites at High Relative Humidity, Mater. Renew. Sust. Ener. 4 (2015) 16.
[17] B. Andreaus, A.J. McEvoy, G.G. Scherer, Analysis of performance losses in polymer electrolyte fuel cells at high current densities by impedance spectroscopy, Electrochim. Acta 47 (2002) 2223–2229.
[18] K.T. Adjemian, S. Srinivasan, J. Benziger, A.B. Bocarsly, Investigation of PEMFC operation above 100 °C employing perfluorosulfonic acid silicon oxide composite membranes, J. Power Sources 109 (2002) 356–364.
[19] L. Rubatat, G. Gebel, O. Diat, Fibrillar Structure of Nafion: Matching Fourier and Real Space Studies of Corresponding Films and Solutions, Macromolecules 37 (2004) 7772.
[20] E. Aleksandrova, R. Hiesgen, K.A. Friedrich, E. Roduner, Electrochemical atomic force microscopy study of proton conductivity in a Nafion membrane, Phys. Chem. Chem. Phys. 9 (2007) 2735.
[21] K.A. Friedrich, M. Schulze, A. Bauder, R. Hiesgen, I. Wehl, X.-Z. Yuan, H. Wang, Nanoscale Investigation of Nafion Membranes after Artificial Degradation, ECS Trans. 25 (2009) 395.
[22] X. Ding, S. Didari, T.F. Fuller, T.A.L. Harris, Effects of Annealing Conditions on the Performance of Solution Cast Nafion Membranes in Fuel Cells, J. Electrochem. Soc. 160 (2013) F793.
[23] A.C.C. Yang, R. Narimani, B.J. Frisken, S. Holdcroft, Investigations of crystallinity and chain entanglement on sorption and conductivity of proton exchange membranes, J. Mem. Sci. 469 (2014) 251.
[24] M. Marechal, J.-L. Souquet, J. Guindet, J.-Y. Sanchez, Solvation of sulphonic acid groups in Nafion® membranes from accurate conductivity measurements, Electrochem. Comm. 9 (2007) 1023.
[25] B.R. Matos, E. Aricó, M. Linardi, A.S. Ferlauto, E.I. Santiago, F.C. Fonseca, Thermal properties of Nafion-TiO_2 composite electrolytes for PEM fuel cell, J. Therm. Anal. Calorim. 97 (2009) 591–594.